Contents

List of Figures

1 Abstract

In the experiment, the average lifetime of the 14,4 keV state of ^{57}Fe is observed. By using the method of delayed coincidences, a time of $\tau = (135 \pm 3)\,\mathrm{ns}$ or $T_{1/2} = (93 \pm 2)\,\mathrm{ns}$ is calculated. To reduce uncertainties, a measurement of random coincidences is made as well as an energy and time calibration.

2 Theory

2.1 Radioactivity

2.1.1 Decay Law

Radioactivity is the property of unstable nuclides to decay by emitting ionising radiation. The process of decay is statistical and the number of nuclides dN which are decaying during a specific amount of time dt is proportional to the number N of existing nuclides.

$$\frac{dN}{dt} = \lambda N. \tag{1}$$

Here, λ is the decay constant. If the number of nucleids at $t = 0$ is given with N_0, the solution of the differential equation gives the decay law

$$N(t) = N_0 \cdot e^{\lambda t}. \tag{2}$$

The half-life $T_{\frac{1}{2}}$ describes the time at which half of the nucleid is decayed. It can be calculated by converting the previous equation into

$$T_{\frac{1}{2}} = \frac{\ln(2)}{\lambda} = \ln 2 \cdot \tau \tag{3}$$

where the mean life-time τ is given by $\tau = \frac{1}{\lambda}$.

2.1.2 Possible Decays

Looking at radioactive decays there are several possible ways for a nucleid to decay.

a **α-Decay:**
If a nucleid emits a Helium nucleid, which consists of two protons and two neutrons, the process is called α-decay. The mass number of the element changes by four, the atomic number by two.

$$^{A}_{Z}X \rightarrow ^{A}_{Z-1}Y + ^{4}_{2}He \tag{4}$$

It is characteristic for heavy nucleids and doesn't have a big impact in the following experiment.

b β^- **-Decay:**
During this process a neutrino becomes a proton by emitting a electron and a electron-antineutrino. The atomic number changes by one.

$$^A_Z X \rightarrow ^A_{Z+1} Y + e^- +$$

c β^+**-Decay:**
Analogue to the previous decay, during this process a proton becomes a neutron. This time a positron and an electron-neutrino are emitted.

$$^A_Z X \rightarrow ^A_{Z-1} Y + e^+ + \nu_e \tag{6}$$

After being slowed down in the material the positron unites with an electron and becomes a positronium. After only a short period of time (around 10^{-9} to 10^{-7}s) the positronium decays into two gamma quants which both have an energy of 511 keV.

d **Electron Capturing (EC):**
The process of electron capturing is a concurrence process to the β^+-decay. The nucleus is able to catch an electron out of the K-shell which combines with a proton and becomes a neutron. A neutrino is emitted and the open spot is filled with an electron from a higher shell, by emitting X-radiation or a Auger-electron. The restocking process continues for shells with a larger distance to the nucleus.

e γ**-Decay:**
This decay happens as a by-product of the processes which were already described. It is high-energetic radiation that is emitted when a nucleus decays into an excited state of its daughter nucleus and then decays into the ground state or a lower energy state. The energy difference is released as gamma radiation.

f **Inner Conversion (IC):** If the energy between the excited state of the daughter nucleus and the lower energy state or the ground state is directly given to an orbital electron (without any emission of radiation), this electron is released and shows a monoenergetic spectrum.

During this experiment the α- and β-decays are almost neglectable, because their radiation is absorbed by the surrounding matter.

2.1.3 Decay Scheme of Cobalt and Americium

For the measurement of the delayed coincidences a ^{57}Co source is used. A ^{241}Am source is used as comparison for the calibration of the spectrum and the energy.

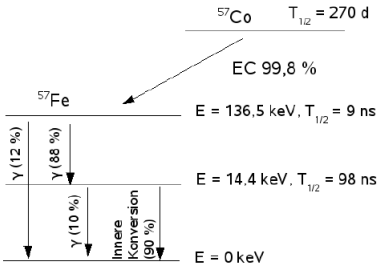

Figure 1: Decay Scheme of Cobalt

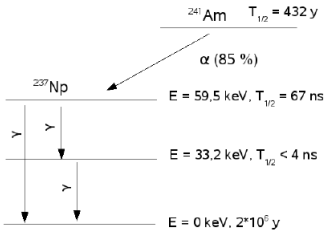

Figure 2: Decay Scheme of Americium

2.1.4 Interdependency of Radiation and Matter

Because gamma quants react as electromagnetic radiation with matter, it is used for their detection. If the gamma quants enter the material with an intensity of I_0 after a distance d it is

$$I_d = I_0 \cdot e^{-\mu d} \tag{7}$$

Here, μ is the absorption coefficient.
There are three different possibilities of interaction:

a **Photo-effect:**
The most dominant effect for energies $E_\gamma < 200$keV is the photo effect where a gamma quant gives all its energy to an electron of the absorber material. If this energy is bigger than the work of emission the electron leaves the atom with kinetic energy and leaves a gap behind. This gap can now be filled with electrons from higher shells which release the energy difference as X-rays or as an Auger-electron.

[b]**Compton-effect:**
This effect happens for energies between energies of 200keV and 5MeV. In this case the gamma quant only transfers a part of its energy to the electron and is scattered. The transmitted energy is dependend on the angle and is at its maximum for 180°.

c **Pair Production:**
The last possibility of interaction is the pair production which only happens for energies higher than 1,022MeV. If a gamma quant enters the electric field of an atom it can be absorbed completely and produce an electron-positron-pair. The remaining momentum is given to the nucleus. Shortly after, the positron and the electron reunite again and decay into two gamma quants with an energy of 511keV. As there are only lower energies during this experiment, it is of no significance.

2.1.5 Characteristics of a Spectrum

In a spectrum there are several peaks which belong to different reactions inside the experiment.

- **Photopeak:**
  This peak shows the energy when the photon that entered the matter gave away all his energy to the molecules.
- **Escapepeak:**
  For the X-radiation it is possible to leave the matter without any interaction. If this happens the energy difference between the two electron levels is lost and the peak is shifted by this amount of lost energy compared to the photopeak.
- **Compton-Edge:**
  When the γ and the electron interact with the compton effect the γ deposes a wide range of different energies in the absorber material. The highest amount of energy which can be deposed due to the compton effect is when they hit at 1801◦. This can be seen as an edge in the measured spectrum (vefore we have a plateau).
- **Backscattering-Peak:**
  γ's which react with the surrounding material of the experiment can depose some of their energy in the surrounding and only the remaining energy inside of the absorber material.
- **X-Ray-Fluoreszenz-Peak:**
  If the γ's depose their energy in the surrounding, only the characteristic X-radiation can be detected.

2.1.6 Measurement Method: Delayed Coincidences

In this experiment the 14,4keV-state of the ^{57}Fe is examined. It arises from the decay of ^{57}Co as it can be seen in 1. As it can be also seen in 1 the process of inner conversion is much more likely to happen for the release of energy of 14,4keV. Therefore, the first signal, the decay from 136,5keV to

14,4keV is delayed by a time T and the second signal, which is the 14,4keV decay is used as the start signal. Thus, the time difference t is not measured directly but $t' = T - t$ and the frequency distribution shows a decreasing curve of decay.

$$N(t') = N_0^{-(T-t)/\tau} \tag{8}$$

Here T is only part of a constant which moves the exponential increase but doesn't influence the life time.

2.1.7 Detection of the γ-Radiation

a **Scintillator:**
During the experiment a anorganic NaI(TI)-szintillator is used. It consists of natrium iodine which is doped with thallium. When a gamma quant enters the matter it gives all or parts of its energy away with the photo- or the compton-effect. The excited electrons are lifted into the conduction band and are afterwards falling back into their ground state by releasing the additional energy. Due to the doping with thallium, there are several possibilities for the electrons to fall to and the emitted light is in the spectrum of visible light.

b **Photomultiplier:**
The photomultiplier changes the received signal of the scintillator in an electrical impulse by hitting electrons out of several photodiodes with the photo-effect. Therefore, the signal is not only changed but also amplified due to secundary electrons.

2.1.8 Used Tools

a **Main Amplifier (MA):**
The main amplifier is used to intensify the received signal and sends it away with less noise than before. The MA has two exits, one which releases a unipolar positive voltage signal and one which releases a bipolar signal that is first positive and after negative. The first one is used to measure spectrums as the entering signal is proportional to the amplitude of the voltage. Due to the zero crossing the second signal is used for critival time measurements.

b **Single Channel Analyzer (SCA):**
At the SCA it is possible to set a higher and a lower border for the amplitude of the impulse and it sends out a signal for each signal it receives inside of this window. Thus, only signals with a defined energy level pass the main amplifier.

c **Time to Amplitude Converter (TAC):**
This device measures the time difference between two signals that

follow each other. The produced suqare pulse is proportional to this measured time difference.

d **Multi Channel Analyzer (MCA):**
The MCA interpretates the spectrums by ordering the different energy levels into channels. With the computer it is possible to create a histogramm.

3 Measurements

3.1 Verification of the Signals with the Oszilloscope

At the beginning of the experiment, the different signals of the devices are checked with the Am sample and the right scintillator. Below the screenshots from the oscilloscope can be seen. From these pictures the timet_d that it took for the signal to decay from 90% to 10% of its intensity is taken. The time t_i, that it took to increase the signal from 10% to 90% is taken out of the figures as well. The results are shown in table 1. However one has to be careful with the pictures, as the signal was fluctuating very much.

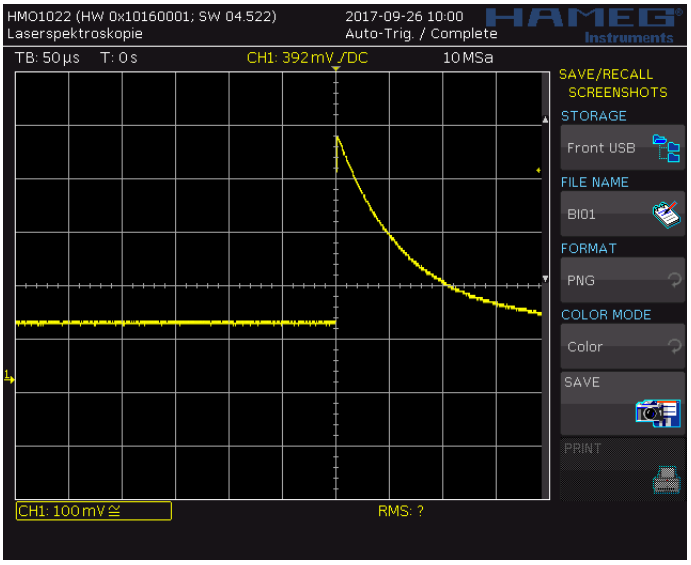

Figure 3: Signal of the Preamplifier

Signal	t_d / μs	t_i / μs
PA	150 ± 40	-
unipolar MA	1,7 ± 0,5	1,1 ± 0,4
bipolar MA	0,9 ± 0,3	1 ± 0,4

Table 1: times measured from the pictures of the oscilloscope

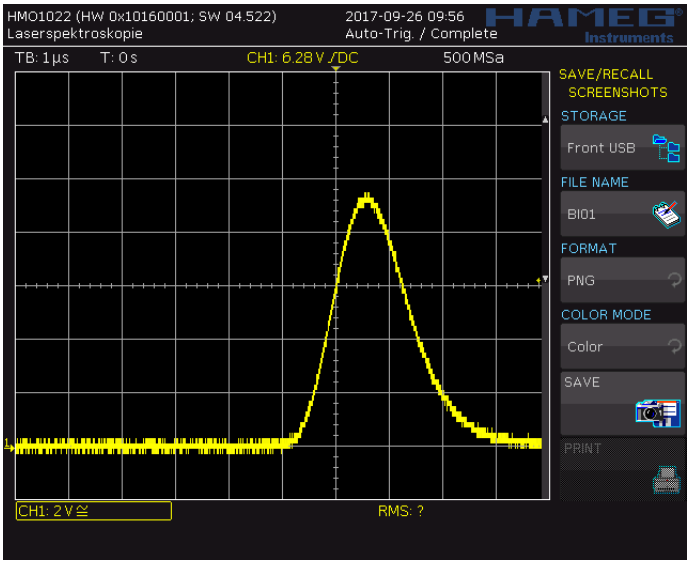

Figure 4: Unipolar Output of the Main Amplifier

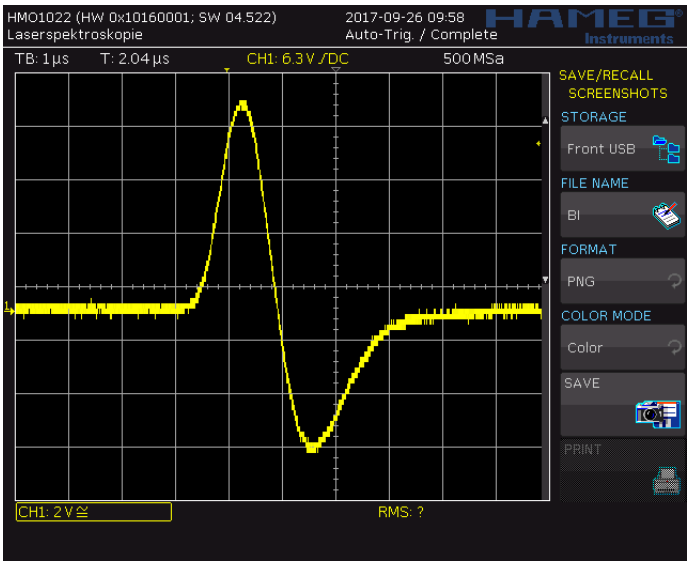

Figure 5: Bipolar Output of the Main Amplifier

3.2 Recording of the Energy Spectra

For the beginning of the measurements for the spectra, the unipolar exit of the Main Amplfier (MA) is connected with the input of the linear gate. The Single Channel Analyser (SCA) connects the bipolar exit of the MA with the Linear Gate (LG). From the LG the signal is transmitted to the Multi Channel Analyser (MCA). Therefore the signal from the unipolar exit of the

MA can only reach the MCA when the signal is in range of the SCA. For the measurement of the whole energy spectrum, the SCA window is fully open. Therefore, the energy-spectrum can be seen in a histogram on the computer.

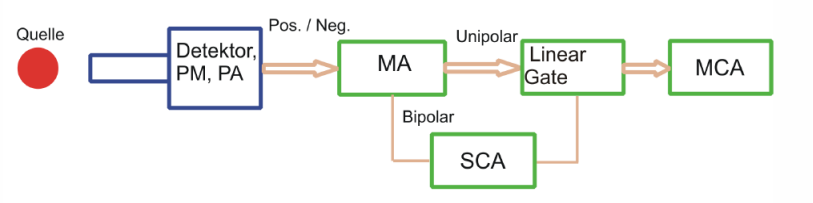

Figure 6: Setup for the Spectra Measurements

First the *Am* sample is put into the device and the spectrum is recorded one time with the left and one time with the right scintillator. The detected spectra are shown in figure 7 and 8.
To determine which one has the better energy resolution, for both visible peaks, a Gaussian fit was made. These Fits are shown together with their fit parameters in figures 16 - 19 in the attachment.
It can be seen, that the peaks of the left scintillator are wider. Its energy resolution is therefore worse.

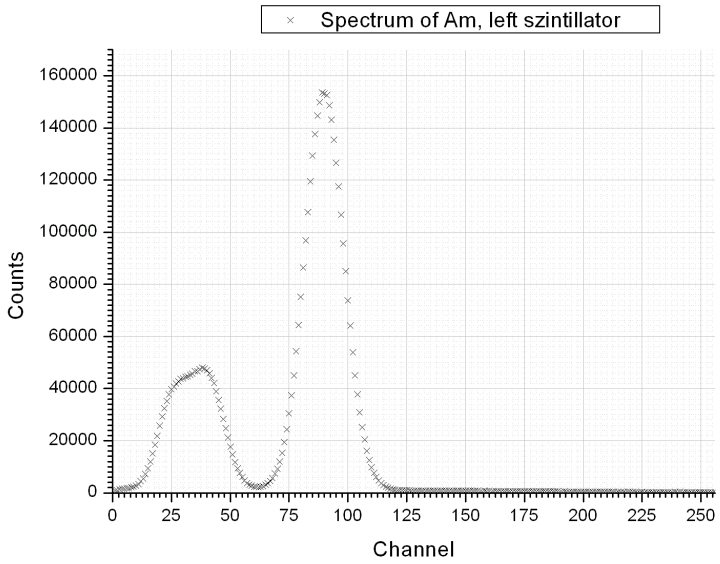

Figure 7: Spectrum of Am, measured with the left scintillator

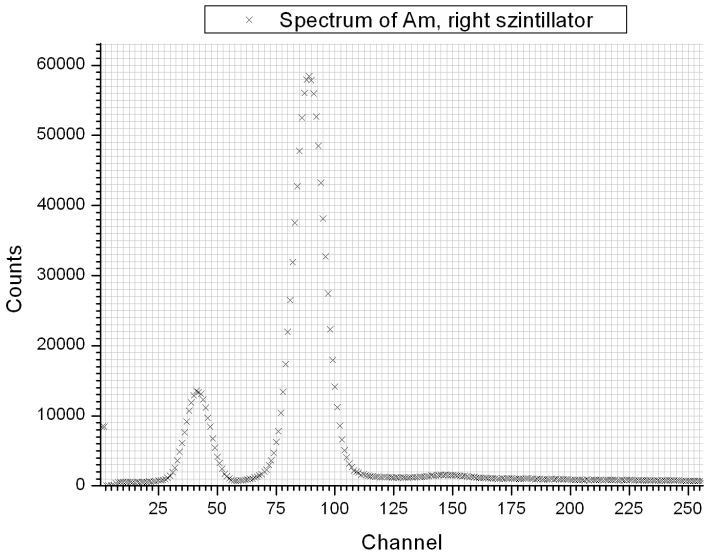

Figure 8: Spectrum of Am, measured with the right scintillator

The hypothesis of the right scintillator having the better energy resolution is supported by the energy spectra detected with Co as a sample. Unfortunately, for the first series of measurements, the Cobalt sample was closed and count rates were therefore smaller than expected.
Figure 9 shows the energy spectrum of the opened cobalt sample measured with the right scintillator. The used windows of the SCA are marked with vertical lines. They are set to For further measurements, the left peak is

left peak		right peak	
min	max	min	max
9	21	157	204

Table 2: Energy windows (in Channels) of the SCA

detected with the right scintillator and the right one with the left scintillator.

3.3 Energy Calibration

The channels of the right hand scintillator should be calibrated with use of the known energies of transitions detected. Those energies can be found in the decay schemes (figures 1 and 2. For americium 3 peaks were expected. However only two of them were detected. In figure 7 it can be seen, that the 33,2 keV and the 26,3 keV transitions overlap. For calculations, the left peak was therefore compared with the arithmetic middle of the energies

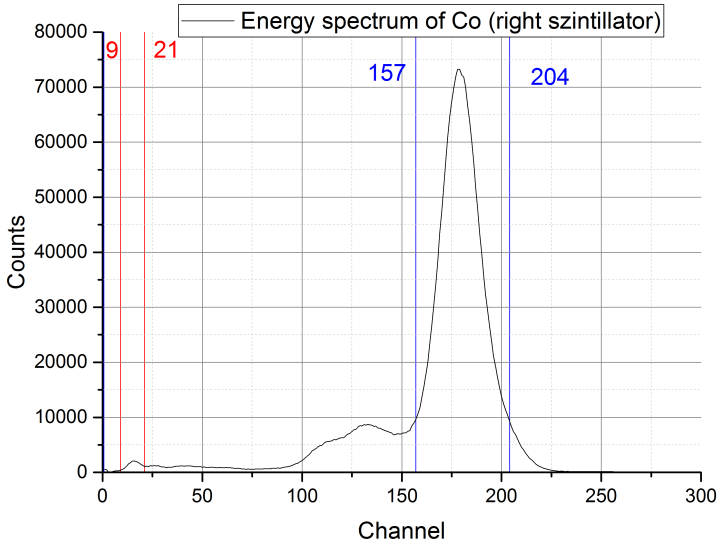

Figure 9: Energy spectrum of Co, right scintillator

(29,7 keV). This is reasonable, since the amount of photons with this energy should be equal, because they are the only ways in and out of the 33,2 keV state.
In figures 18 - 21 the position of the peak is determined from a Gaussian fit for each peak.
With the positions and according energies, a linear regression is made. The regression is shown in figure 22 in the appendix. The data used is shown in table 3.

Channel	Energy / keV
16,26	14,4
41,729	29,7
89,068	59,5
179,36	122

Table 3: Data used for the energy calibration fit

The fit gave the following results

y_0 / s	s_{y_0} / s	a / s	s_a / s	Kor. R-Quadrat
2,4	1,4	0,662	0,013	0,99871

Table 4: Results of the linear regression for energy calibration

This leaves us with an Energy of $(0,662 \pm 0,013)$ **keV per channel.**

3.4 Time Calibration

For calibration of the Time to Amplitude Converter (TAC), a setting shown in figure 10 is used. Therefore, the amplification was set, so that a maximum delay of 190,5 ns resulted in a channel output in the middle of the spectrum. In steps of 32 ns, the delay was reduced and the channel where a signal appeared was measured. The last step was only a reduction by 16 ns.
In figure 11 the adjusted delay is plotted over the Channel where a signal was detected. With those values, a linear regression is made. The results are shown in table 6. The exact data points are listed in table 5

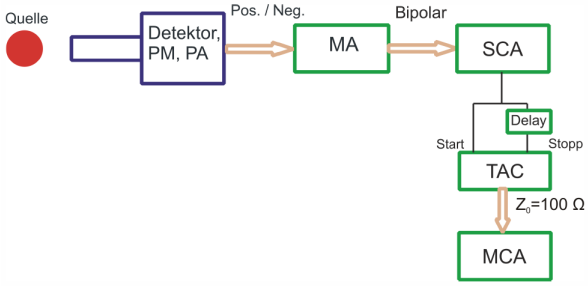

Figure 10: Setup for time calibration

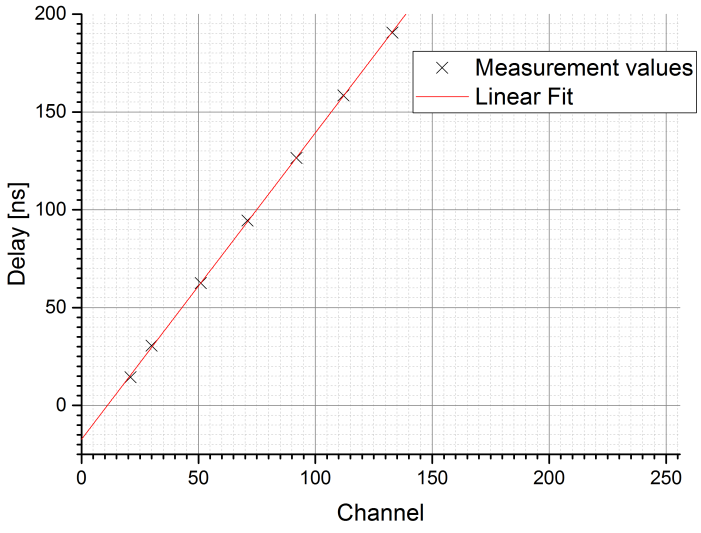

Figure 11: Linear Fit for time calibration

Delay / ns	Channel
14,5	21
30,5	30
62,5	51
94,5	71
126,5	92
158,5	112
190,5	133

Table 5: Data of the linear regression for time calibration

y_0 / s	s_{y_0} / s	a / s	s_a / s	Kor. R-Quadrat
-17,3	0,6	1,566	0,007	0,99987

Table 6: Results of the linear regression for time calibration

3.5 Background measurement

The measurement of delayed coincidences measures the time difference between the 14,4 keV transition and the 122 keV transition that has been delayed by 190,5 ns. It can happen that those two transitions do not come from the same atom and give therefore an unintened count. To reduce this uncertainty, the same setup and energy windows as for the main measurement are used. The only difference is, that the delay is not on the 122 kev signal, but on the 14,4 keV signal. Therefore, the stop signal does surely not come from the same atom.
The resulting time distribution after a measurement time of $t_u = 10932$ s is shown in figure 12. The error bars come from the underlying Poisson distribution and are given as $\sqrt{N}$

It can be seen, that there is a peak for a low channel number, which means, that there are a lot of short times measured. For channels >26 the background seems even. To verify this, a linear regression was made. The results are shown in tabular 7. It can be seen, that the inclination does not vary significantly from zero. That's why the Underground can be taken as constant Offset in case all measurements below channel 26 are ignored.

y_0	s_{y_0}	a	s_a	Kor. R-Quadrat
0,30	0,09	$3{,}6 \cdot 10^{-4}$	$5{,}8 \cdot 10^{-4}$	-0,00265

Table 7: Results of the linear regression for background measurement

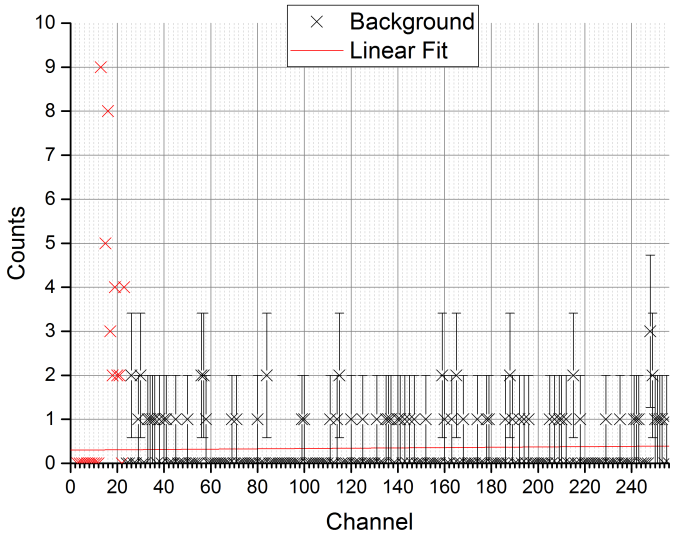

Figure 12: Backgroundmeasurement (10932 s)

3.6 Measurement of delayed coincidences

This is the main measurement from which the lifetime of the 14,4 keV state of Fe is calculated. The setup is shown in figure 13. As a maximum delay, 190,5 ns is used. The energy windows of the SCA are set as described in table 2. With a measurement time of $t_m = 54812$ s, the calculated Offset for the background has to be rescaled.
The new offset is

$$y_{Off} = \frac{t_m}{t_u} \cdot y_0 = 1,5 \tag{9}$$

$$s_{y_{Off}} = y_{Off} \cdot \frac{s_{y_0}}{y_0} = 0,5 \tag{10}$$

Therefore, $y_{Off} = 1,5 \pm 0,5$ has to be subtracted from the counts in each channel. The uncertainty on the number of Counts follows as

$$N = N_{mess} - y_{Off} \tag{11}$$

$$s_N = \sqrt{N_{mess} + 0,5^2} \tag{12}$$

The corrected Counts are plotted in figure 14 over their according channels. Due to decay law this looks like a rising exponential function. It rises because of the swaped start and stop signal. This leads to a mirroring on the y-axis.

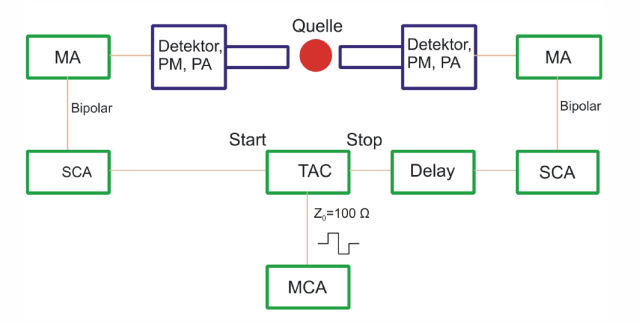

Figure 13: Setup for the measurement of delayed coincidences

3.6.1 Exponential Fit

To get the average lifetime τ_c, the following function is fitted on the data. The number of the channel is described with C

$$N = N_0 \cdot e^{\frac{C}{\tau_c}} \tag{13}$$

Because of the information given by the background measurement, channels smaller than 26 are ignored for the fit as well as values where the counts were getting smaller for higher channels. Ignored values are marked red. The fit gives the following results:

N_0	s_{N_0}	τ_c	s_{τ_c}	Kor. R-Quadrat
4,5	0,2	86	2	0,87274

Table 8: Fiting results of the exponential fit

This value has to be converted to a time using the time calibration. With the constant $a = 1,566 \pm 0,007$ calculated in table 6, the average lifetime τ and half-time period $T_{1/2}$ is given as

$$\tau = a \cdot \tau_c = 135 \text{ ns} \tag{14}$$

$$s_\tau = \tau \cdot \sqrt{\left(\frac{s_a}{a}\right)^2 + \left(\frac{s_{\tau_c}}{\tau_c}\right)^2} = 3 \text{ ns} \tag{15}$$

$$T_{1/2} = \ln(2) \cdot \tau = 93 \text{ ns} \tag{16}$$

$$s_{T_{1/2}} = \ln(2) \cdot s_\tau = 2 \text{ ns} \tag{17}$$

So the final result is

$$\boxed{\tau = (135 \pm 3)\,\text{ns}} \tag{18}$$

$$\boxed{T_{1/2} = (93 \pm 2)\,\text{ns}} \tag{19}$$

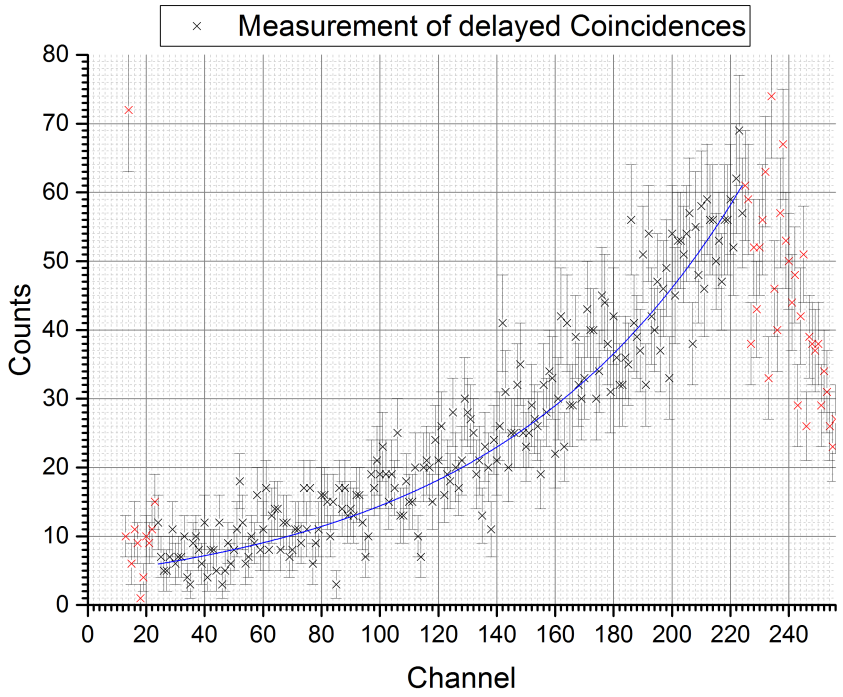

Figure 14: Exponential fit for the corrected measurement of delayed coincidences (54812 s)

3.6.2 Linear Fit

In addition a linear fit on an logarithmic y-axis should be made. Figure 15 shows the exact same data as figure 14, but has the logarithm taken for the counts. As an exponential behaviour of the original data is expected, a linear fit is made. The results are shown in table 9.

y_0	s_{y_0}	a	s_a	Kor. R-Quadrat
1,52	0,05	0,0117	0,0004	0,79196

Table 9: Results of the linear regression for the delayed coincidences with logarithmic counts

To get τ from the inclination, the reciprocal value of the inclination has

to be calculated. The further analysis is analogous to the exponential fit.

$$\tau_c = \frac{1}{a} = 85 \tag{20}$$

$$s_{\tau_c} = \tau_c \cdot \frac{s_a}{a} = 3 \tag{21}$$

This leads to

$$\boxed{\tau = (134 \pm 5)\,\mathrm{ns}} \tag{22}$$

$$\boxed{T_{1/2} = (93 \pm 3)\,\mathrm{ns}} \tag{23}$$

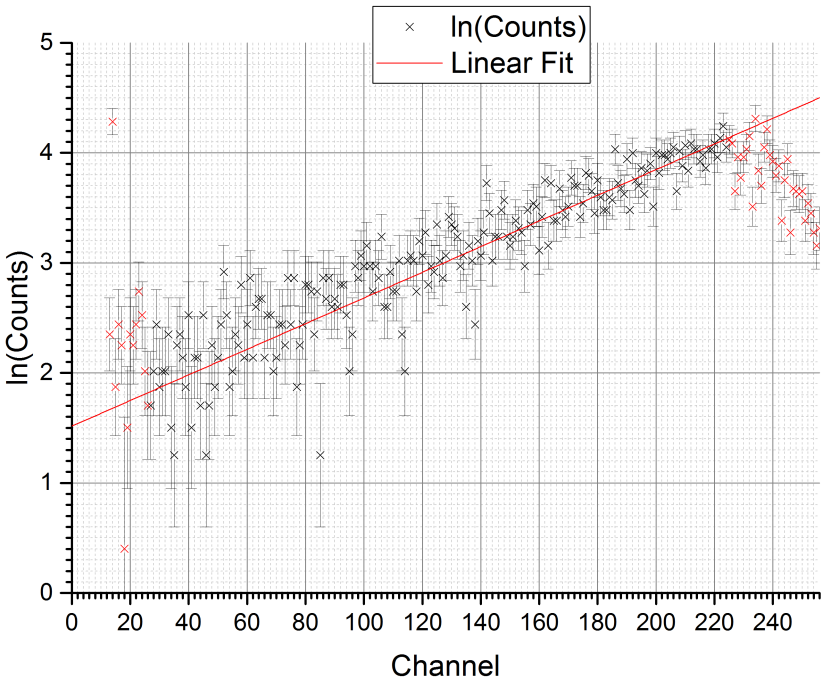

Figure 15: Linear fit for the corrected measurement of delayed coincidences (logarithmic Counts) (54812 s)

4 Discussion

As average lifetime for the 14,4 keV of ^{57}Fe, a time of

$$\textbf{Exponential Fit:} \quad \boxed{\tau = (135 \pm 3)\,\text{ns}} \tag{24}$$

could be calculated using an exponential fit function. A linear fit on a logarithmic y-axis resulted in

$$\textbf{Linear Fit:} \quad \boxed{\tau = (134 \pm 5)\,\text{ns}} \tag{25}$$

Those two values are within 1 standard deviation of each other. However this is not surprising, because the same data was used for both fits. In fact, they are expected to be equal. The remaining difference is reasoned in the different fit functions that were used by Origin. This result shows, that it is better to use an exponential function, because the resulting uncertainties are smaller.
The coefficient of determination is with 0,87274 relatively near to 1. That confirms the expectation of a rising exponential function.
As a half-life period, a time of

$$\textbf{Exponential Fit:} \quad \boxed{T_{1/2} = (93 \pm 2)\,\text{ns}} \tag{26}$$

$$\textbf{Linear Fit:} \quad \boxed{T_{1/2} = (93 \pm 2)\,\text{ns}} \tag{27}$$

is calculated. With the linear fit the uncertainty is 1 ns bigger. They are directly calculated from τ, which means that everything said to τ applies for $T_{1/2}$ as well.
The literature value for $T_{1/2}$ given in the instruction is

$$T_{1/2lit} = 98\,\text{ns} \tag{28}$$

For the exponential fit, the literature value is in range of 3 standard deviations. For the linear fit it is even in range of 2 standard deviations. This shows that there has to be a small systematic offset that hasn't been respected yet.
The time calibration of the TAC showed that the linear regression had a significant y Offset, which means that small channels represent negative time differences. Or in other words, the channel that represents no time difference has a channel number larger than 0.
Enabling Offsets in x and y direction could change the fit parameter τ. Looking at figure 11 shows that the Offset in x direction caused by time calibration could be around 11 channels.
However, looking at the exponential plot (figure 14), we can see that there are far bigger offsets than the one caused by time calibration.

The 14,4 keV transition starts the time measurement and the 122 keV transition stops it. Still, the 122 keV transition has happened before. If the average lifetime was 0 ns (only hypothetical), the measured time would exactly be the delay, that is placed behind the SCA of the 122 keV signal. For longer lifetimes, some of the delay time has already past before the 14,4 keV signal is detected and the resulting time measured by the TAC is smaller.
This means, we expect the highest possible channel, that measures counts to be in the area of the highest delay from the time calibration.
This has been at channel 133, whereas the highest Counts of the measurement are around channel 220. This is a shift by 87 channels, that can not be explained by time calibration and is likely to have the higher impact on the final result.
Influences of random coincidences were mostly erased by a background measurement. By only looking at a specific part of the time spectrum it was made sure, that the background is relatively even. Higher measurement times would reduce uncertainties.
Due to small windows around the characteristic peaks of the transitions, the background was further reduces at the cost of less data points.

5 Attachment

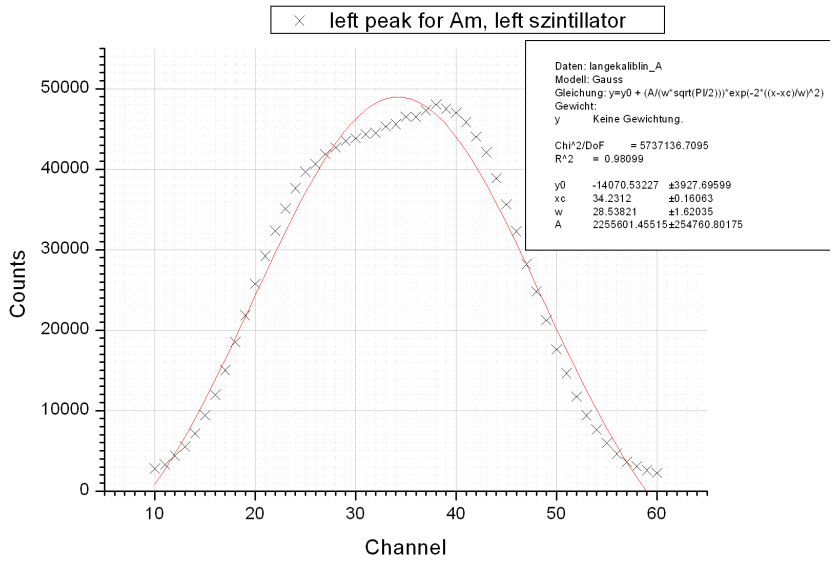

Figure 16: Measurement of Am, left scintillator, left peak

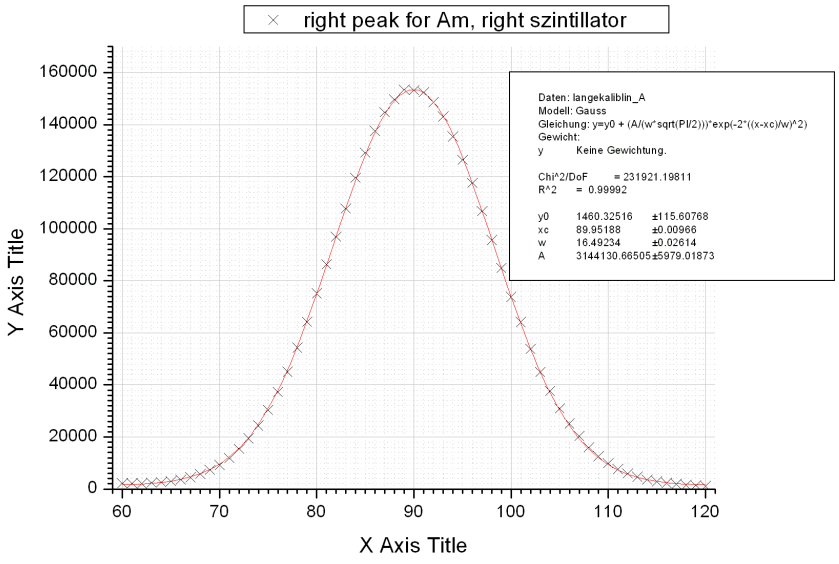

Figure 17: Measurement of Am, left scintillator, right peak

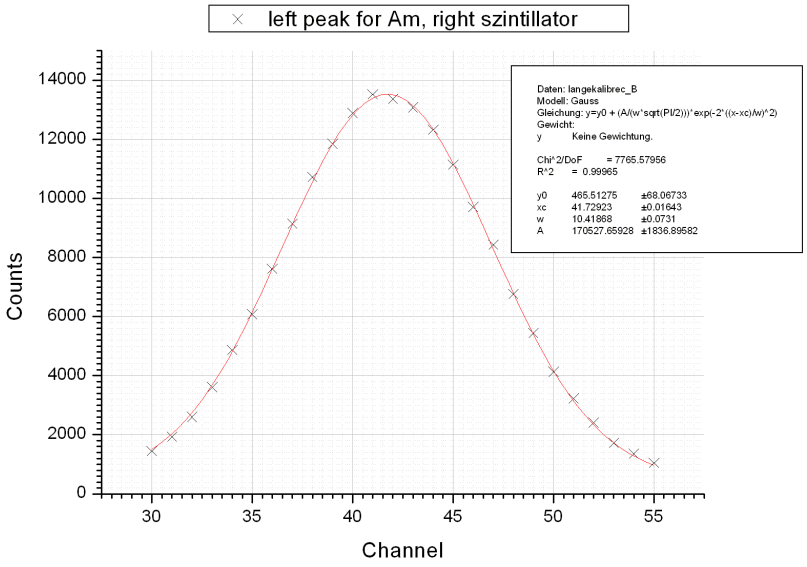

Figure 18: Measurement of Am, right scintillator, left peak

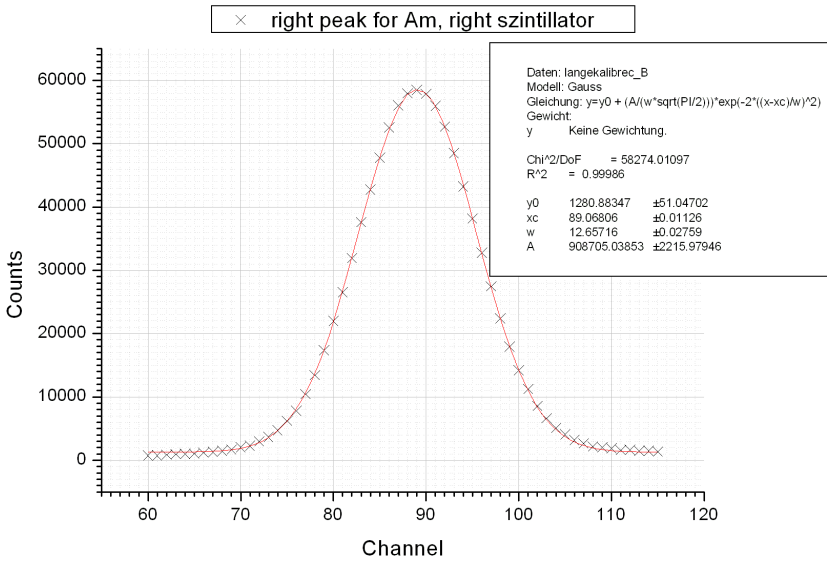

Figure 19: Measurement of Am, right scintillator, right peak

$y0$	s_{y0}	xc	s_xc	w	s_w	A	s_A	Kor. R-Quadrat
7475	429	179,36	0,06	18,3	0,2	$150{,}7{\cdot}10^4$	$2{,}3{\cdot}10^4$	0,99668

Table 10: Fit parameters for Co, right scintillator, right peak

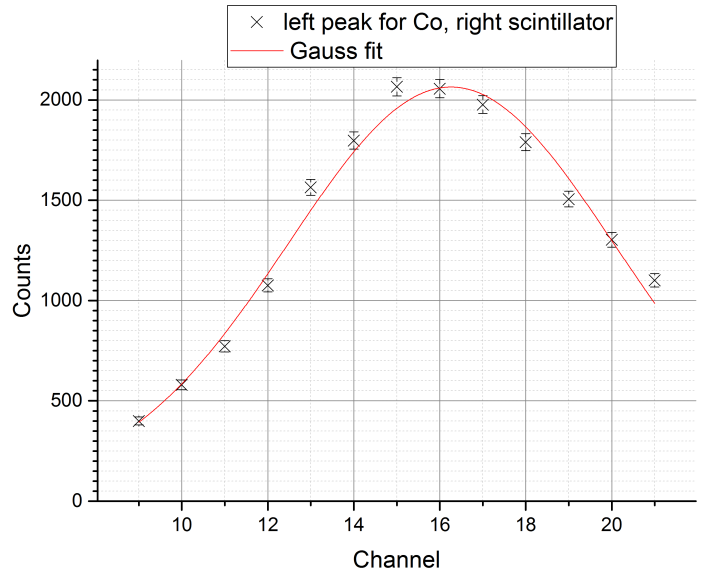

Figure 20: Measurement of Co, right scintillator, left peak

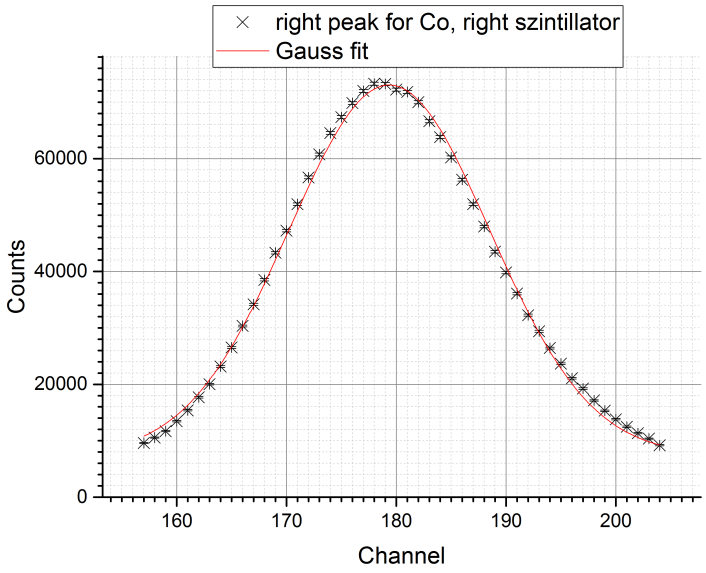

Figure 21: Measurement of Co, right scintillator, right peak

$y0$	s_{y0}	xc	$s_x c$	w	s_w	A	s_A	Kor. R-Quadrat
74	146	16,26	0,10	7,6	0,6	18933	2633	0,9838

Table 11: Fit parameters for Co, right scintillator, left peak

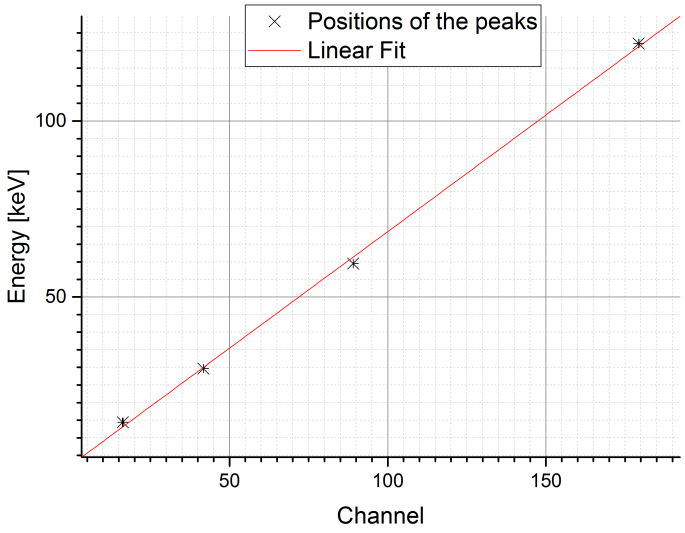

Figure 22: Linear fit for the energy calibration of the right hand scintillator